









Original scientific paper

## Scaling-ion removal from high-salinity produced water *via* sono-electrocoagulation: interplay of floc microstructure and electrochemical surface activity

Reno Pratiwi<sup>1,✉</sup> , Kartika Fajarwati Hartono<sup>1</sup> , Maman Djumantara<sup>1</sup> ,  
Dina Asmaul Chusniyah<sup>1,2</sup> , Wiwik Dahani<sup>3</sup>  and Tiur Elysabeth<sup>4</sup> 

<sup>1</sup>Petroleum Engineering Department, Faculty of Earth and Energy Technology, Universitas Trisakti, Jalan Letjen S. Parman 1, Jakarta 11440, Indonesia

<sup>2</sup>Institute of Geology and Geophysics, Chinese Academy of Science, University of Chinese Academy of Science, Beijing 100029, China

<sup>3</sup>Mining Engineering Department, Faculty of Earth and Energy Technology, Universitas Trisakti, Jalan Letjen S. Parman 1, Jakarta 11440, Indonesia

<sup>4</sup>Department of Chemical Engineering, Faculty of Engineering, Universitas Serang Raya, Serang 42162, Indonesia

Corresponding Author: ✉ [reno.pratiwi@trisakti.ac.id](mailto:reno.pratiwi@trisakti.ac.id); Tel.: +62-823-2204-6787

Received: January 27, 2026; Revised: March 26, 2026; Published: April 5, 2026

### Abstract

Produced water from oil fields contains complex dissolved organic and inorganic species, including  $\text{Ca}^{2+}$ ,  $\text{HCO}_3^-$ , and  $\text{CO}_3^{2-}$ , which induce  $\text{CaCO}_3$  scaling and hinder waterflooding operations. This study investigated the performance of electrocoagulation (EC) and ultrasonic-assisted electrocoagulation (sono-EC) for treating native produced water from Indonesian oil fields, focusing on scaling ion removal, floc structural characteristics, and hydrogen evolution. Experiments were conducted at pH 5, 7 and 9 using Al-SS316 electrodes under constant current conditions, with intermittent sonication applied to enhance  $\text{Al}^{3+}$  release and suppress electrode passivation. The results demonstrated that pH 7 provides optimal conditions for the formation of stable amorphous  $\text{Al}(\text{OH})_3$  flocs. Scanning electron microscopy analysis revealed a porous lamellar morphology that promotes ion adsorption and co-precipitation, resulting in the highest removal efficiencies of  $\text{Ca}^{2+}$ ,  $\text{HCO}_3^-$  and chemical oxygen demand (COD). Sonication further enhanced process performance by inducing cavitation-driven micro-mixing, accelerating floc growth, and increasing hydrogen evolution. Brunauer-Emmett-Teller and Barrett-Joyner-Halenda analyses confirmed pronounced pH-dependent differences in floc porosity and surface characteristics, which mechanistically explained variations in ion capture behaviour. Overall, the sono-EC operated at neutral pH offers an effective strategy to mitigate scaling potential, while hydrogen evolution is used as an electrochemical indicator of cathodic surface activity.

## Keywords

Produced water pollutants; electrochemical removal; ultrasonic treatment; scale causing ions; flocs characterization; hydrogen evolution; cavitation depassivation; Faradaic efficiency.

---

## Introduction

Produced water from the oil and gas industry is the largest waste product, accounting for approximately 80 to 90 % of total production volume. The complex composition of produced water poses significant challenges due to organic contaminants and high inorganic ions such as  $\text{Ca}^{2+}$ ,  $\text{HCO}_3^-$ , and  $\text{CO}_3^{2-}$  [1-3]. Among these challenges, the presence of carbonate-associated ions is of particular concern, as they promote the formation of calcium carbonate ( $\text{CaCO}_3$ ) scale [4,5], a major cause of decreased injectivity, fouling, and equipment failure in many oil fields. A large volume of produced water is often reinjected into the reservoir to aid production, maintain pressure, or support waterflooding. This makes effective scale precursor removal through wastewater treatment essential for long-term operational reliability [6].

Recently, electrocoagulation (EC) has gained significant attention as a wastewater treatment method that can destabilize organic and inorganic pollutants without chemical coagulants. When aluminium electrodes are employed, this process generates aluminium hydroxide flocs *in situ*, which act as effective coagulants for destabilizing dissolved and colloidal pollutants. Although several studies have explored the removal of chemical oxygen demand (COD), turbidity, dyes, and heavy metals using EC [7-9], only a few have investigated its performance in removing scale ions such as  $\text{Ca}^{2+}$ ,  $\text{HCO}_3^-$ , and  $\text{CO}_3^{2-}$ , despite their direct relevance to oil and gas fields. Most existing reports also rely on synthetic water or focus primarily on organic degradation. This creates a significant knowledge gap regarding the performance of EC in real produced water matrices, where ionic equilibria, buffering effects, and competitive reactions differ substantially from those in laboratory-prepared systems.

One of the EC process developments carried out is a hybrid method that incorporates ultrasonic waves into EC (sono-EC). This method has been shown to increase mass transfer, reduce electrode passivation, promote micro-mixing, and enhance the degradation of organic pollutants through cavitation-driven oxidation [10-13]. The current literature on sono-EC still focuses significantly on organic removal, leaving a substantial knowledge gap regarding the effects on scale-causing ion removal, floc formation dynamics, and the stability of aluminium hydroxide species under various pH conditions. There is a lack of studies that mechanistically correlate ultrasonic cavitation with the structural and morphological changes in flocs produced by EC, particularly in the high-salinity environments characteristic of produced water.

Although pH-driven aluminium speciation, including transitions between  $\text{Al}^{3+}$ ,  $\text{Al}(\text{OH})_2^+$ ,  $\text{Al}(\text{OH})_3(\text{s})$  and  $\text{Al}(\text{OH})_4^-$ , is well understood [14-18], limited studies have related these transformations to quantitative floc porosity data. Understanding how pH and sonication influence coagulants, including specific surface area and pore-size distribution, is essential for determining floc capacity to adsorb and encapsulate dissolved ions. Currently, reports on Brunauer-Emmett-Teller (BET) characterization of electrocoagulated flocs are limited, particularly in real-world produced water treatment systems. Therefore, this study presents a systematic evaluation of EC and sono-EC performance in removing scale-causing ions and organic contaminants from real produced water sourced from active oil fields in Indonesia. In the context of produced water management, scaling potential evaluation is generally focused on the concentrations of  $\text{Ca}^{2+}$ ,  $\text{HCO}_3^-$  and  $\text{CO}_3^{2-}$  ions because their interaction controls the carbonate-bicarbonate equilibrium that determines the level of supersaturation and precipitation of calcium carbonate ( $\text{CaCO}_3$ ). Based on the chemical characterization of the produced water used in this

study, the carbonate system shows a dominant concentration compared to other scale-forming ions, so monitoring  $\text{Ca}^{2+}$ ,  $\text{HCO}_3^-$  and  $\text{CO}_3^{2-}$  can be used as the main indicators of scale formation potential in the studied system. This is because these three ions are the main precursors of calcium carbonate ( $\text{CaCO}_3$ ) scale formation, globally recognized as the most common type of scaling occurring in oil wells, fluid processing facilities, and reinjection systems [19]. The formation of  $\text{CaCO}_3$  reaction is highly dependent on the interaction of  $\text{Ca}^{2+}$ ,  $\text{HCO}_3^-$  and  $\text{CO}_3^{2-}$  ions through the carbonate-bicarbonate equilibrium, which determines the supersaturation level and tendency for precipitation [20,21]. Previous studies have shown that the presence of  $\text{Mg}^{2+}$ ,  $\text{Ba}^{2+}$  or  $\text{SO}_4^{2-}$  ions is relevant in the case of gypsum ( $\text{CaSO}_4$ ) or barite ( $\text{BaSO}_4$ ) scaling, which are not dominant in the composition of produced water in many Indonesian oil fields, including the water source used in this study [1,5].

In addition to assessing process effectiveness, this study provides new insights into how pH conditions and ultrasonic treatment affect the formation, morphology, and porosity characteristics of coagulants. The analysis is conducted using an integrative approach combining scanning electron microscopy (SEM) and BET analysis. Furthermore, hydrogen evolution during the EC process is quantitatively examined to show potential as a valuable byproduct in water treatment. By combining process performance evaluation and material characterization, this study offers a robust mechanistic framework to explain how operational parameters influence coagulant properties and pollutant removal effectiveness. The results are expected to provide significant scientific guidance for optimizing EC-based technologies for produced water management and scale mitigation.

## Materials and methods

### Produced water characteristic

Produced water samples were obtained from the Cepu Oil Field, Central Java. The characteristics observed during the EC process are shown in Table 1.

**Table 1.** Produced water characteristics

Concentration, g L <sup>-1</sup>				pH
Ca <sup>2+</sup>	HCO <sub>3</sub> <sup>-</sup>	CO <sub>3</sub> <sup>2-</sup>	COD	
13	2.074	0.177	1.400	9

As an observed variable, the pH of the sample solution was adjusted using 1 M NaOH or 1 M HCl to obtain pH levels of 5, 7 or 9, representing acidic, neutral and basic solution conditions, respectively.

### Electrocoagulation process

The EC process was carried out in a 250 mL batch reactor with an aluminium electrode plate as the anode and a 316 stainless steel plate as the cathode, each measuring 2 cm × 4 cm, with a distance of 3 cm. Both electrodes were connected to a direct current of 0.4 A and maintained for 60 minutes. Stirring was performed in the process to maintain homogeneity, minimize passivation and fouling, and accelerate gas release from the solution.

### Ultrasonic-assisted electrocoagulation

Ultrasonic-assisted electrocoagulation was conducted by integrating intermittent ultrasonic irradiation into the conventional EC process to enhance mass transfer and mitigate electrode passivation. Sonication was performed using an ultrasonic bath (model MH-020S, China) operating at a fixed frequency of 40 kHz and a nominal power of 120 W. The electrocoagulation reactor was placed inside the ultrasonic bath to allow indirect ultrasonic exposure, ensuring uniform cavitation throughout the solution while avoiding direct mechanical erosion associated with probe-type sonicators.

Sonication was applied intermittently, consisting of 5 minutes of ultrasonic irradiation followed by 10 minutes without sonication, repeatedly throughout the total EC duration of 60 minutes. This operational mode was selected to balance cavitation-induced enhancement effects with floc stability and energy efficiency. During non-sonicated intervals, electrocoagulation proceeded under identical electrical and hydrodynamic conditions as the conventional EC experiments.

The primary function of sonication in this system was to promote cavitation-driven micro-mixing, facilitate the release of  $\text{Al}^{3+}$  ions from the anode surface, enhance contact between coagulant species and dissolved ions, and suppress the formation of passive oxide layers on the aluminium electrode. The influence of ultrasonic irradiation was evaluated by comparing process performance, floc characteristics, and hydrogen evolution under sonicated and non-sonicated conditions at identical pH values.

### *Analytical methods*

Samples were collected at 15-minute intervals during the electrocoagulation process and analysed immediately to minimize post-treatment chemical changes. Calcium ion ( $\text{Ca}^{2+}$ ) concentration was determined using complexometric EDTA titration, following standard analytical procedures. Bicarbonate ( $\text{HCO}_3^-$ ) and carbonate ( $\text{CO}_3^{2-}$ ) concentrations were quantified by acid-base titration using standard alkalinity determination methods, allowing differentiation between the carbonate and bicarbonate species based on the titration endpoints.

Chemical oxygen demand (COD) was measured using the closed reflux colorimetric method in accordance with Standard Methods for the Examination of Water and Wastewater (APHA 5220D) [22]. All measurements were conducted in triplicate, and average values are reported to ensure analytical reliability. Solution pH was monitored using pH universal indicator throughout the experiments.

Hydrogen gas generated during the electrocoagulation process was collected volumetrically at the end of the 60-minute operation period. The concentration of hydrogen in the produced gas was measured using a gas chromatograph (Shimadzu GC-2014) equipped with a molecular sieve (MS) 5A column, using argon as the carrier gas, with a known retention time. The experimentally measured hydrogen yield was compared with the theoretical hydrogen production calculated from Faraday's law to determine Faradaic efficiency, which was used as an indicator of cathodic electrochemical activity under different operating conditions.

### *Coagulant characterization*

The surface morphology of flocculant granules and aluminium plates, as well as the morphology and surface characteristics of electrocoagulated flocs and aluminium electrode surfaces, were characterized using field-emission scanning electron microscopy/energy-dispersive X-ray spectroscopy (FESEM/EDX) (Thermo Fisher Scientific - Prisma E-SEM, USA) in high vacuum mode with 4,500x to 10,000x magnifications, and an accelerating voltage of 10 to 12 kV; the spot size was set at 2.5 (instrument setting). This analysis was conducted to evaluate floc morphology and electrode surface characteristics and confirm assumptions based on previous results [1,10], and to assess floc structure, lamellar features, surface roughness and electrode surface changes associated with passivation and depassivation phenomena.

The combined SEM and BET- Barrett-Joyner-Halenda (BJH) analyses were used to correlate floc morphology and porosity with pH conditions and ultrasonic treatment, providing mechanistic insight into the relationship between floc microstructure, ion adsorption capacity, and electrochemical process performance.

## Results and discussion

The discussion of the mechanistic aspects of the EC and sono-EC processes is developed by linking pH-influenced aluminium speciation, floc microstructure, and electrode surface activity. These three variables are assessed as interrelated in determining process performance, particularly in terms of their ability to eliminate scaling ions and hydrogen evolution, the latter being used as an indicator of the extent to which electrical charge can be utilized under constant current operation.

An efficient method, such as EC, capable of simultaneously addressing the complexities of inorganic and organic components, is required to treat produced water from the oil and gas industry. Therefore, this study observed the performance of aluminium-based EC, showing its ability to produce in-situ flocs as adsorbents for dissolved pollutants, alongside hydrogen gas as a co-benefit. The challenges encountered included anode passivation, floc instability at certain pH values, and limited aluminium decay as the base material for  $\text{Al}(\text{OH})_3$  floc formation. Although the integration of sonication has been proposed to improve EC performance, previous literature has reported inconsistent results and has neglected fundamental interactions among sonication, pH, aluminium speciation, and floc structure [23-25].

In this study, the integration of ion analysis, COD, hydrogen evolution, SEM morphology, and pore characterization using BET and BJH provided new insights into how pH and sonication synergistically influence floc quality and treatment efficiency. The results showed that pH was a critical factor in determining aluminium speciation and controlling the physicochemical properties of flocs.

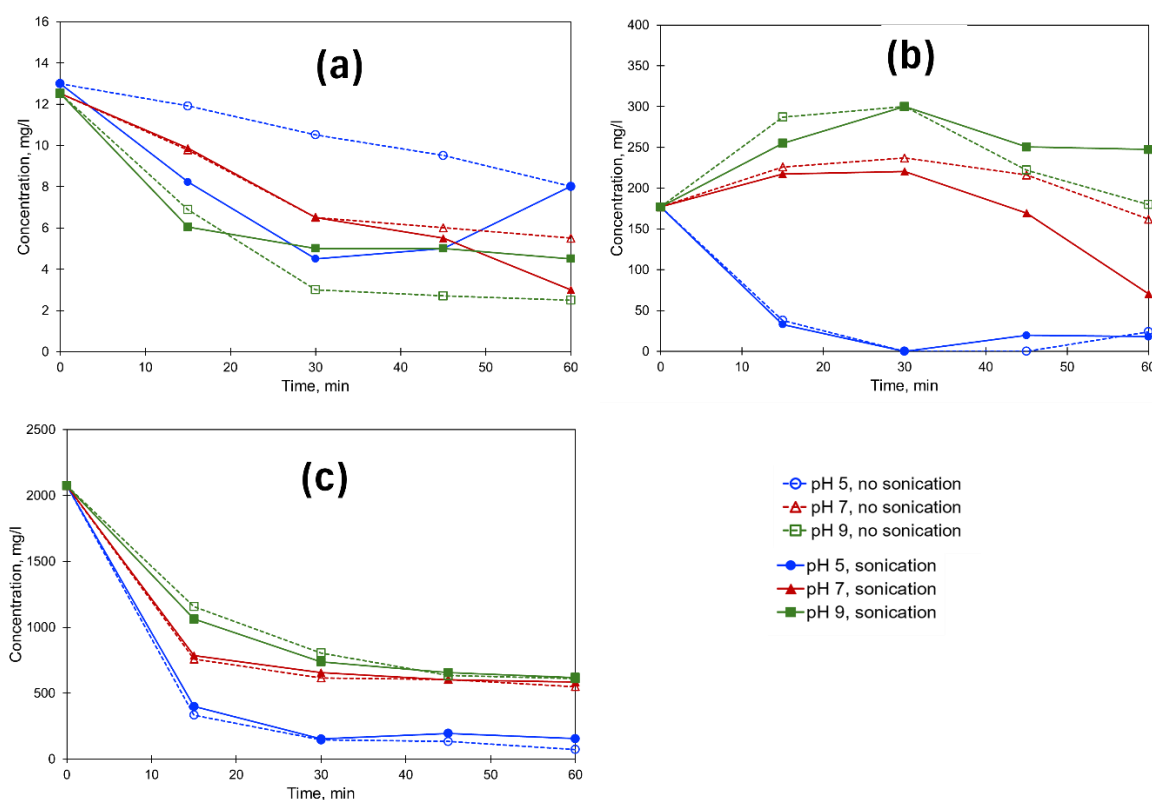


**Figure 1.** Changes in the concentrations of (a)  $\text{Ca}^{2+}$ , (b)  $\text{CO}_3^{2-}$  and (c)  $\text{HCO}_3^-$  ions in produced water during EC process at various pH values and with sonication/non-sonication treatments

The acidic condition at a pH of 5 causes aluminium species to be dominated by  $\text{Al}^{3+}$ ,  $\text{Al}(\text{OH})_2^+$  and  $\text{Al}(\text{OH})_3$ , which are soluble, reactive, and unstable as solid coagulants. Therefore, the flocs formed tended to be brittle and easily broken, and they had the potential to re-release previously adsorbed ions. At pH 5, the carbonate system also experiences a significant equilibrium shift, where  $\text{CO}_3^{2-}$  and  $\text{HCO}_3^-$  are protonated to form  $\text{H}_2\text{CO}_3$ , which decomposes to form dissolved  $\text{CO}_2$ . The mechanism is enhanced by cavitation turbulence due to sonication, which accelerates  $\text{CO}_2$  stripping from the

solution. This led to a rapid decrease in carbonate-bicarbonate ion concentration with and without sonication, as shown in Figure 1. For  $\text{Ca}^{2+}$ , sonication yields a clear performance improvement, as evidenced by the significantly lower final  $\text{Ca}^{2+}$  concentration compared to the unsonicated condition. The observed variation was attributed to high formation of reactive Al-hydrolysis clusters capable of capturing  $\text{Ca}^{2+}$  despite the instability of the floc. In comparison, the effect of sonication on  $\text{CO}_3^{2-}$  and  $\text{HCO}_3^-$  at pH 5 was relatively small, as most of the reduction was due to chemical  $\text{CO}_2$  formation rather than the coagulation mechanism. BET analysis results in Figure 2 showed that the pores in floc at pH 5 were relatively large but not interconnected. This indicates that under acidic conditions, floc is less mechanically stable and prone to collapse, as reported by Cañizares *et al.* [26] and Jo *et al.* [27].

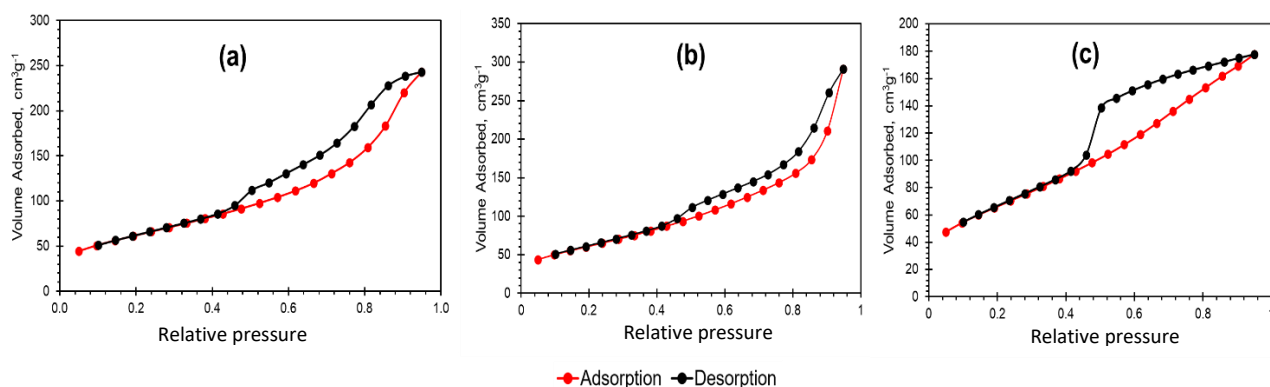


**Figure 2.** The results of BET analysis of flocs that occurred from EC process performed successively at (a) pH 5, (b) pH 7 and (c) pH 9

In a neutral solution at pH 7, the dominant aluminium species is amorphous  $\text{Al}(\text{OH})_3$ , which is the most effective form for adsorption and sweep flocculation. Flocs formed under these conditions are stable, porous, and have a strong lamellar character, as presented in the SEM image in Figure 3.

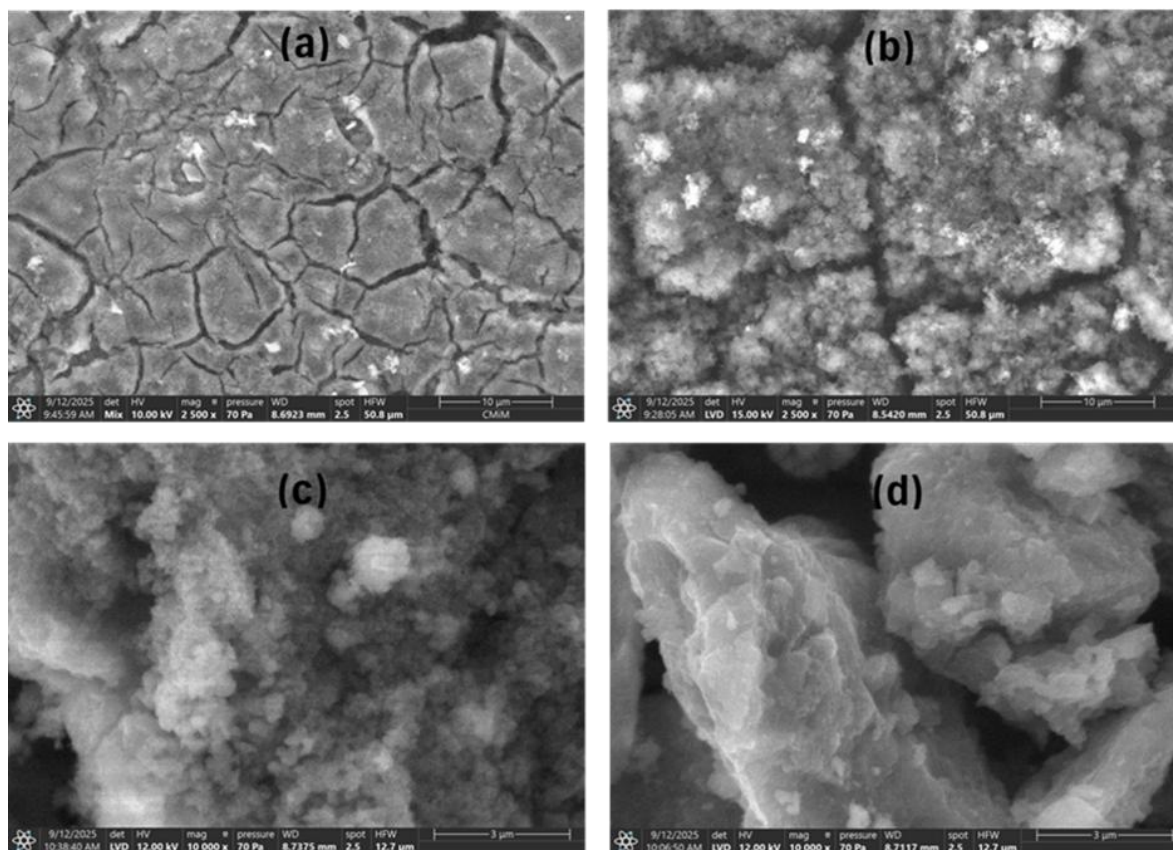


**Figure 3.** SEM characterization results for aluminum plate surface (a) without sonication and (b) with sonication; coagulant surface (c) without sonication and (d) with sonication at pH 7

Furthermore, BET results showed a more interconnected pore structure, providing active sites for interaction with  $\text{Ca}^{2+}$  ions and carbonate-bicarbonate anions. This mechanism is consistent with previous studies, in which sweep flocculation by  $\text{Al}(\text{OH})_3$  was reported to be effective when the floc was at optimal pH conditions [15,28]. In terms of the performance shown in Figure 1, the decreases in  $\text{Ca}^{2+}$  and  $\text{HCO}_3^-$  concentrations were significant and relatively stable over time. For  $\text{CO}_3^{2-}$ , the effect of sonication was most pronounced, where treatment without sonication caused a moderate decrease in  $\text{CO}_3^{2-}$ . Meanwhile, sonication treatment showed a significant further decrease after 30 minutes. This indicated that pH 7 did not provide the greatest reduction for all scaling ions but offered the most balanced combination of removal efficiency and floc stability.

Different results were obtained under alkaline conditions (pH 9), where the abundance of  $\text{OH}^-$  ions allowed aluminium species to form  $\text{Al}(\text{OH})_4^-$ , a soluble form that could not generate sufficient amounts of solid coagulant. Therefore, the produced flocs were small, non-cohesive, and low-porosity. Previous studies reported that excessively high pH levels prevented aluminium from forming a soluble complex and hindered the contribution to the sweeping mechanism [29]. As presented in Figure 1, the reduction in scaling ions at pH 9 was significantly lower, while the BET analysis in Figure 2 showed a minimum pore volume.

To further clarify the role of pH and sonication treatment in the EC process, Table 2 displays the BET-BJH textural parameters of electrocoagulated flocs. BET surface areas were calculated from adsorption data in the relative pressure range  $P/P_0 = 0.05$  to  $0.30$ . Total pore volume was estimated at  $P/P_0 \approx 0.99$ , and average pore diameter was derived from BJH desorption analysis.

**Table 2.** Properties of EC flocs under different pH and sonication conditions

Process condition	BET surface area, $\text{m}^2 \text{g}^{-1}$	Total pore volume, $\text{cm}^3 \text{g}^{-1}$	Average pore diameter, nm
pH 5, no sonication	226.96	0.38	3.31
pH 7, no sonication	225.91	0.45	4.00
pH 9, no sonication	243.16	0.28	2.26
pH 7, sonication	209.91	0.28	2.45
pH 9, sonication	224.77	0.22	1.94

Table 2 reveals that the maximum floc surface area was observed at pH 9, although this condition did not correspond to the lowest values of total pore volume and pore diameter. This suggests the formation of compact, non-cohesive microflocs at pH 9, attributable to the predominance of  $\text{Al}(\text{OH})_4^-$  species under alkaline conditions, which hinder the development of sweep floc structures. In contrast, at neutral pH, flocs exhibited higher pore volume and pore diameter, consistent with the formation of amorphous  $\text{Al}(\text{OH})_3$  species. BET analysis further indicates that these flocs possess an interconnected and open pore network, providing abundant active sites for ion adsorption and facilitating efficient mass transfer at the liquid-electrode interface, thereby enhancing the removal of scale-forming ions.

Table 2 also highlights the impact of sonication, which consistently reduced floc surface area, pore volume, and average pore diameter across all pH conditions. This phenomenon is attributed to cavitation-induced micro-fragmentation, which generates smaller lamellar structures and disrupts fragile pore frameworks. At neutral pH, sonication appears to refine  $\text{Al}(\text{OH})_3$  flocs characterized by inherently stronger structures into more uniformly distributed porous units, thereby improving their capacity to sweep dissolved contaminants. This interpretation is corroborated by the progressive decline in dissolved Ca concentration (Figure 1) and COD values (Figure 4), which demonstrate sustained removal efficiency at pH 7. Conversely, under alkaline conditions, electrochemical performance was limited due to the formation of fragile flocs with minimal porosity.

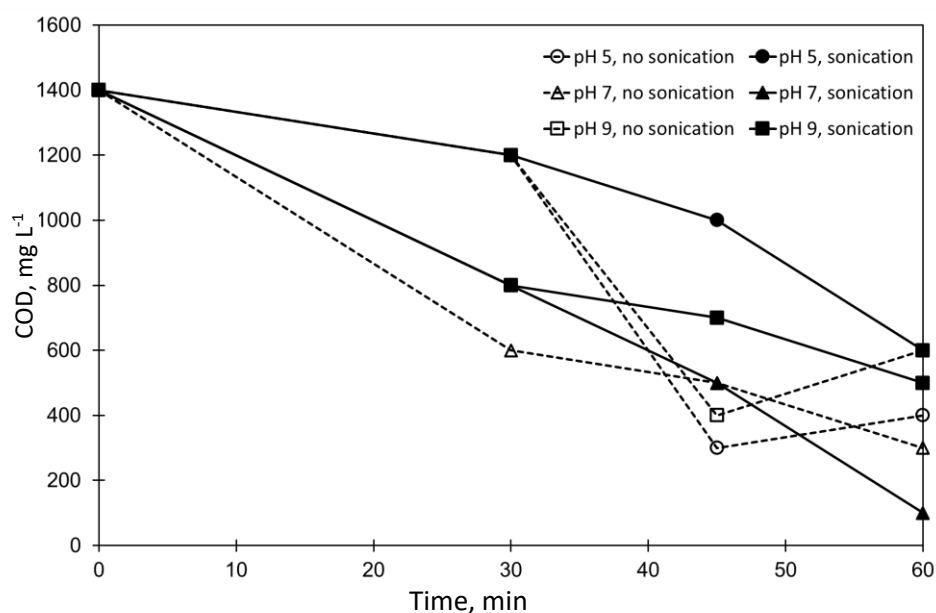


**Figure 4.** Changes in COD values of produced water under various EC process conditions

The integration of sonication introduced physicochemical phenomena not found in conventional EC. Specifically, sonication produced cavitation, the formation and collapse of microbubbles, causing high local pressure, microstreaming, and intense turbulence at the microscale [30]. This cavitation effect accelerates mass transfer, improves mixing homogeneity, and promotes the release of  $\text{Al}^{3+}$  ions from the anode. Various studies reported that the contact probability between coagulant and contaminant was increased by introducing turbulence, particularly in solutions with high ionic content, such as produced water [31,32]. This study also indicated that sonication functioned as an effective depassivation mechanism. SEM images of the electrode showed a rough, inhomogeneous surface, filled with micro-pits after sonication, indicating the erosion of the passive  $\text{Al}_2\text{O}_3$  oxide layer. The result suggests that, in addition to its hydrodynamic role, sonication improves electrochemical efficiency by reducing the anode surface resistance. Previous electrochemical studies on sono-electrolysis systems have shown similar phenomena [31,33].

At pH 5, sonication provided a significant benefit for  $\text{Ca}^{2+}$  removal but altered significant  $\text{CO}_3^{2-}$  and  $\text{HCO}_3^-$  reduction trends. A slight rebound in carbonate concentration at the end of the reaction suggests that fragmentation of fragile flocs can trigger some back-release, although overall removal performance is high. At pH 9, due to limited coagulant formation, sonication provided no significant benefit and likely only increased energy requirements. These results show that sonication does not automatically improve EC performance under all conditions, although its effectiveness must be considered in relation to aluminium speciation and floc stability.

The advantages of sonication were significant at pH 7, where  $\text{Al}(\text{OH})_3$  floc has high structural integrity. Under these conditions, the micro-fragmentation process produced by cavitation did not damage the floc but refined it into layered units to increase active surface area. BET showed increased pore connectivity after sonication, while BJH indicated a more defined mesopore distribution. Furthermore, SEM images showed a cleaner, smoother, and more uniform lamellar structure. This transformation indicates that sonication could increase mesoporosity in certain hydroxide materials. The improved floc structure showed a significant increase in  $\text{Ca}^{2+}$ ,  $\text{HCO}_3^-$  and  $\text{CO}_3^{2-}$  removal at pH 7 during sonication.

COD removal performance followed a similar trend. As presented in Figure 4, the combination of adsorption by porous flocs and oxidation of hydroxyl radicals ( $\bullet\text{OH}$ ) generated by cavitation significantly reduced COD at pH 7, as also reported by Gogate and Pandit [34]. At pH 5, the fragile, unstable floc easily

released the captured organic compounds, leading to inconsistent COD reduction. The low coagulant formation was the main cause of the inefficiency of adsorption at pH 9. Consequently, the role of sonication was limited only to the partial breakdown of organics by free radicals.

Hydrogen production in the EC process serves as a practical indicator of the cathodic electrochemical activity, reflecting both electrode surface conditions and bubble dynamics influenced by sonication. Figure 5 shows the hydrogen yield after 60 minutes of electrocoagulation at different pH values, with and without sonication. The bar plots represent the experimentally measured hydrogen yield, while the line plots indicate the corresponding Faradaic efficiency (FE), calculated from the theoretical hydrogen yield based on Faraday's law. For the applied current of 0.4 A and operation time of 60 min, the theoretical hydrogen amount was estimated as 7.46 mmol *per run*, based on Equation (1):

$$n_{\text{H}_2, \text{theo}} = \frac{It}{2F} \quad (1)$$

The hydrogen amount was then converted to the Faraday efficiency (FE) to quantify the fraction of the applied charge that contributes to the cathodic hydrogen evolution reaction.

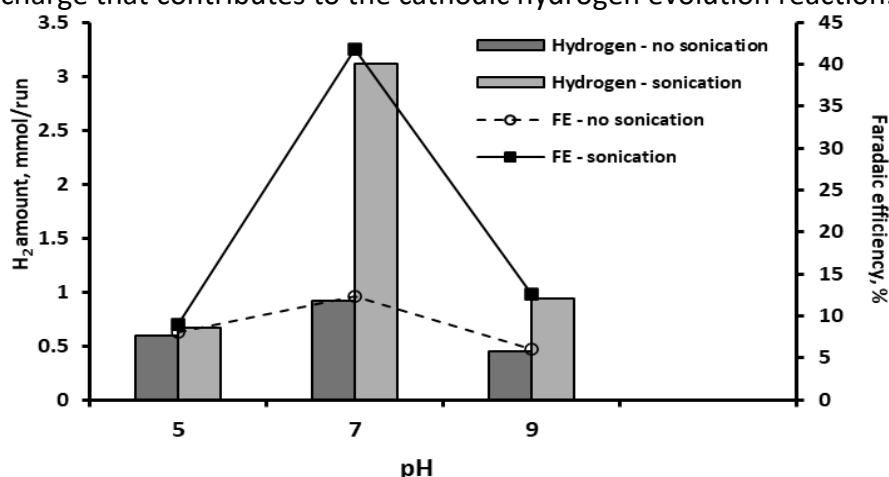


**Figure 5.** Hydrogen amount per run and Faradaic efficiency at various pH under different EC process conditions

As shown in Figure 5, conventional EC exhibited relatively low FE values (6 to 12 %), indicating that a significant portion of the applied current was consumed by side processes or hindered by mass-transfer limitations and bubble coverage at the cathode surface. The introduction of sonication substantially increased the FE, particularly at neutral pH, where the efficiency rose from 12.35 to 41.81 %. This improvement suggests that ultrasonic cavitation facilitated faster detachment of hydrogen bubbles and reduced diffusion resistance near the cathode, thereby enhancing the effective utilization of the applied current for hydrogen evolution.

The pronounced pH dependence of FE further underscores that cathodic activity is tightly coupled to the physicochemical conditions governing floc formation and electrode-surface interactions. At pH 7, maximum hydrogen evolution is achieved because three conditions are simultaneously met. These include the stable release of  $\text{Al}^{3+}$  ions, flocs that do not disrupt the cathode surface, and high water-reducing activity due to depassivation. Sonication accelerates the release of hydrogen bubbles, thereby reducing diffusion barriers and increasing reaction efficiency. A recent sono-electrolysis study demonstrated a similar phenomenon, indicating that cavitation can accelerate gas release from the cathode surface [35]. At pH 5 and 9, floc instability and low coagulant settling have little impact on sonication during hydrogen production.

In the treatment of produced water known for its high salinity, the stability of the flocs produced during the electrocoagulation process will impact electrode surface conditions. At neutral pH, stable and porous  $\text{Al}(\text{OH})_3$  flocs are produced, thus minimizing surface coverage and floc fragmentation.

The formed flocs settle more readily in the bulk solution. This condition results in a more reduced electrode passivation, thereby enhancing electrochemical efficiency through sustained  $\text{Al}^{3+}$  ion release. At the same time, limited floc clogging facilitates faster gas bubble evolution on the cathode surface, which is reflected in higher FE values. Conversely, under acidic and basic solution conditions, floc formation tends to be unstable and insufficient, respectively. These conditions lead to more rapid electrode surface clogging and limited depassivation, resulting in lower cathodic activity. This combined effect indicates that floc stability, anodic depassivation, and cathodic activity are intrinsically interconnected in high-salinity matrices.

It should be emphasized that hydrogen measurements were performed only at the end of the process (after 60 minutes), serving solely as a metric for comparing relative cathodic effectiveness across pH conditions and sonication treatments. Consequently, these endpoint data do not provide insights into the kinetics of hydrogen evolution.

The observed trends indicate that electrocoagulation performance in high-salinity produced water is governed by a coupled interaction between aluminium hydrolysis behaviour, floc microstructure, and electrode surface conditions. Neutral pH favours the formation of stable  $\text{Al}(\text{OH})_3$  flocs with interconnected porosity, while ultrasonic irradiation modifies mass transfer and electrode surface states through cavitation-induced effects. However, the extent to which sonication enhances treatment efficiency is strongly dependent on floc stability and aluminium speciation, as evidenced by the contrasting behaviour observed under acidic and alkaline conditions. These results emphasize that electrochemical performance, ion removal efficiency, and hydrogen evolution cannot be interpreted independently but must be evaluated as interconnected physicochemical processes within the electrocoagulation system.

## Conclusions

The results obtained show that pH 7 is the most rational operating condition for EC-sonication systems applied to produced water. This pH value offers an optimum compromise between coagulant chemistry, pore structure, adsorption capacity, floc mechanical stability, electrochemical efficiency, and hydrogen production. For oil and gas industry applications, this configuration has important practical implications, as produced water intended for reuse as an injection fluid must exhibit sufficiently low concentrations of  $\text{Ca}^{2+}$ ,  $\text{CO}_3^{2-}$ , and  $\text{HCO}_3^-$  to minimize the risk of calcium carbonate scaling in reservoir formations. The results demonstrate that the combination of pH 7 and sonication significantly reduces the concentration of scaling ions while producing stable and easily separable flocs, thereby enabling safer waterflooding operations. In addition, hydrogen evolution serves as a robust indicator of cathodic electrochemical activity under varying pH and sonication conditions.

**Conflict of interest:** *The authors declare that there are no conflicts of interest regarding the publication of this paper. All funding and support received have not influenced the design, execution, or conclusions.*

**Acknowledgements:** *This study was financially supported by the Ministry of High Education, Research, and Technology of the Republic of Indonesia (Kemendikristek RI) under the Fundamental Regular Research Grant with the contract number 124/C3/DT.05.00/PL/2025, 1014/LL3/AL.04/2025, 493/A/LPPM/USAKTI/VI/2025.*

**Funding:** *This study was financially supported by the Ministry of High Education, Research, and Technology of the Republic of Indonesia (Kemendikristek RI) under the Fundamental Regular Research Grant with the contract number 124/C3/DT.05.00/PL/2025, 1014/LL3/AL.04/2025, 493/A/LPPM/USAKTI/VI/2025.*

## References

- [1] F. Al-Ajmi, M. Al-Marri, F. Almomani, Electrocoagulation Process as an Efficient Method for the Treatment of Produced Water Treatment for Possible Recycling and Reuse, *Water* **17** (2025) 23. <https://doi.org/10.3390/w17010023>
- [2] A. Kadier, Z. Al-Qodah, G. K. Akkaya, D. Song, J. M. Peralta-Hernandez, J.Y. Wang, C. Phalakornkule, M. Bajpai, N. M. Niza, V. Gilhotra, M. E. Bote, Q. Ma, C. C. Obi, C. A. Igwegbe, A state-of-the-art review on electrocoagulation (EC): An efficient, emerging, and green technology for oil elimination from oil and gas industrial wastewater streams, *Case Studies in Chemical and Environmental Engineering* **6** (2022) 100274. <https://doi.org/10.1016/j.cscee.2022.100274>
- [3] H. I. Eldos, M. Khan, N. Zouari, S. Saeed, M. A. Al-Ghouti, Characterization and assessment of process water from oil and gas production A case study of process wastewater in Qatar, *Case Studies in Chemical and Environmental Engineering* **6** (2022) 100210. <https://doi.org/10.1016/j.cscee.2022.100210>
- [4] M. Piccioli, S. V. Aanesen, H. Zhao, M. Dudek, G. Øye, Gas flotation of petroleum produced water: A review on status, fundamental aspects, and perspectives, *Energy and Fuels* **34** (2020) 15579-15592. <https://doi.org/10.1021/acs.energyfuels.0c03262>
- [5] K. T. Amakiri, A. R. Canon, M. Molinari, A. Angelis-Dimakis, Review of oilfield produced water treatment technologies, *Chemosphere* **298** (2022) 134064. <https://doi.org/10.1016/j.chemosphere.2022.134064>
- [6] C. Abdelhamid, A. Latrach, M. Rabiei, K. Venugopal, Produced Water Treatment Technologies: A Review, *Energies* **18** (2025) 63. <https://doi.org/10.3390/en18010063>
- [7] S. Boinpally, A. Kolla, J. Kainthola, R. Kodali, J. Vemuri, A state-of-the-art review of the electrocoagulation technology for wastewater treatment, *Water Cycle* **4** (2023) 26-36. <https://doi.org/10.1016/j.watcyc.2023.01.001>
- [8] J. Taumaturgo, M. A. Ormeno, C. J. Meza, G. M. Cuadros, L. A. C. Venegas, C. A. A., Dextre, O. J. R. Taranco, C. A. Carhuaricra, P. D. Bravo, J. A. M. Pisfil, Processes Coupled to Electrocoagulation for the Treatment of Distillery Wastewaters, *Sustainability* **16** (2024) 6383. <https://doi.org/10.3390/su16156383>
- [9] F. Y. AlJaberi, Z. A. Hawaas, Electrocoagulation removal of Pb, Cd, and Cu ions from wastewater using a new configuration of electrodes, *MethodsX* **10** (2022) 101951. <https://doi.org/10.1016/j.mex.2022.101951>
- [10] S. O. A. Nassar, M. S. Yusoff, H. Halim, N. H. M. Kamal, M. J. K. Bashir, T. S. B. A. Manan, H. A. Aziz, A. Mojiri, Ultrasonic (US)-Assisted Electrocoagulation (EC) Process for Oil and Grease (O&G) Removal from Restaurant Wastewater, *Separations* **10** (2023) 61. <https://doi.org/10.3390/separations10010061>
- [11] N. Vukojević Medvidović, L. Vrsalović, S. Svilović, S. Gudić, I. Čule, Sono-and Zeolite-Assisted Electrocoagulation for Compost Wastewater Treatment: Does Ultrasound Power Make a Difference?, *Minerals* **14** (2024) 1190. <https://doi.org/10.3390/min14121190>
- [12] H. Posavcic, I. Halkijevic, D. Vouk, M. Cvetnic, Circulating flow hybrid ultrasonic and electrochemical process for the treatment of mineral oil wastewaters, *Journal of Water Process Engineering* **49** (2022) 103024. <https://doi.org/10.1016/j.jwpe.2022.103024>
- [13] N. Al-rubaiey, M. Al-Barazanji, Ultrasonic Technique in Treating Wastewater by Electrocoagulation, *Engineering and Technology Journal* **36** (2018) 54-62. <http://dx.doi.org/10.30684/etj.36.1C.9>
- [14] M. Malakootian, N. Yousefi, The efficiency of electrocoagulation process using aluminum electrodes in removal of hardness from water, *Iranian Journal of Environmental Health Science and Engineering* **6** (2009) 131-136. <https://scispace.com/pdf/the-efficiency-of-electrocoagulation-process-using-aluminum-4p4jtj78g9.pdf>
- [15] A. S. Naje, S. Chelliapan, Z. Zakaria, M. A. Ajeel, A review of electrocoagulation technology for the treatment of textile wastewater, *Reviews in Chemical Engineering* **33** (2017) 263-292. <https://doi.org/10.1515/revce-2016-0019>
- [16] R. Pratiwi, S. Slamet, R. Muttaqin, D. S. Dilla, The opportunity of using hydrogen produced from electrocoagulation process of hospital liquid waste as renewable energy source, *AIP Conference Proceedings* **2667** (2023) 030006. <https://doi.org/10.1063/5.0115636>
- [17] A. Gasmi, S. Ibrahim, N. Elboughdiri, M. A. Tekaya, D. Ghernaout, A. Hannachi, A. Mesloub, B. Ayadi, L. Kolsi, Comparative Study of Chemical Coagulation and Electrocoagulation for the Treatment of Real Textile Wastewater: Optimization and Operating Cost Estimation, *ACS Omega* **7** (2022) 22456-22476. <https://doi.org/10.1021/acsomega.2c01652>

- [18] M. A. Madhavan, S. P. Antony, Effect of polarity shift on the performance of electrocoagulation process for the treatment of produced water, *Chemosphere* **263** (2021) 128052. <https://doi.org/10.1016/j.chemosphere.2020.128052>
- [19] K. Ramstad, K. Sandengen, A. F. Mitchell, E. Moldrheim, Correlating calcium carbonate scale risk with field experience data, *Society of Petroleum Engineers - SPE International Oilfield Scale Conference and Exhibition, 2025*, SPE-224279-MS. <https://doi.org/10.2118/224279-MS>
- [20] J. Wang, X. Gao, Z. Li, Y. Wang, C. Gao, CaCO<sub>3</sub> scaling of oilfield produced water in 'electrochemical pre-oxidation-coagulation sedimentation-filtration' process: reason, mechanism, and countermeasure, *Desalination Water Treat* **57** (2016) 12415-12423. <https://doi.org/10.1080/19443994.2015.1054313>
- [21] C. Zhang, T. Cai, S. Ge-Zhang, P. Mu, Y. Liu, J. Cui, Wood Sponge for Oil-Water Separation, *Polymers* **16** (2024) 2362. <https://doi.org/10.3390/polym16162362>
- [22] APHA, Standard Methods for the Examination of Water and Wastewater, 23<sup>rd</sup> ed., 2017. <https://dokumen.pub/standard-methods-for-the-examination-of-water-and-wastewater-23th-23thnbsped-9780875532875.html>
- [23] X. Ma, Z. Wang, Removal of Ciprofloxacin from Wastewater by Ultrasound/Electric Field/Sodium Persulfate (US/E/PS), *Processes* **10** (2022) 124. <https://doi.org/10.3390/pr10010124>
- [24] A. K. Verma, R. R. Dash, P. Bhunia, A review on chemical coagulation /flocculation technologies for removal of colour from textile wastewaters, *Journal of Environmental Management* **93** (2012) 154-168. <https://doi.org/10.1016/j.jenvman.2011.09.012>
- [25] Z. Bachari, A. A. Isari, H. Mahmoudi, S. Moradi, E. H. Mahvelati, Application of natural surfactants for enhanced oil recovery - critical review, *IOP Conference Series: Earth and Environmental Science* **221** (2019) 012039. <https://doi.org/10.1088/1755-1315/221/1/012039>
- [26] P. Cañizares, C. Jiménez, F. Martínez, M. A. Rodrigo, C. Sáez, The pH as a key parameter in the choice between coagulation and electrocoagulation for the treatment of wastewaters, *Journal of Hazardous Materials* **163** (2009) 158-164. <https://doi.org/10.1016/j.jhazmat.2008.06.073>
- [27] S. Jo, R. Kadam, H. Jang, D. Seo, J. Park, Recent Advances in Wastewater Electrocoagulation Technologies: Beyond Chemical Coagulation, *Energies* **17** (2024) 5863. <https://doi.org/10.3390/en17235863>
- [28] A. R. Anuf, K. Ramaraj, V. S. Sivasankarapillai, R. Dhanusuraman, J. P. Maran, G. Rajeshkumar, A. Rahdar, A. M. Diez-Pascual, Optimization of electrocoagulation process for treatment of rice mill effluent using response surface methodology, *Journal of Water Process Engineering* **49** (2022) 103074. <https://doi.org/10.1016/j.jwpe.2022.103074>
- [29] Y. Ullah, X. He, Y. Fang, J. Lu, A review about flocs in electrocoagulation process: Generation, adsorption, transformation, transportation, *Process Safety and Environmental Protection* **202** (2025) 107452. <https://doi.org/10.1016/j.psepp.2025.107452>
- [30] J. Madhavan, J. Theerthagiri, D. Balaji, S. Sunitha, Ultrasound: An Overview, *Molecules* **24** (2019) 3341. <https://doi.org/10.3390/molecules24183341>
- [31] C.-C. He, C.-Y. Hu, S.-L. Lo, Evaluation of sono-electrocoagulation for the removal of Reactive Blue 19 passive film removed by ultrasound, *Separation and Purification Technology* **165** (2016) 107-113. <https://doi.org/10.1016/j.seppur.2016.03.047>
- [32] K. Song, Y. Liu, A. Umar, H. Ma, H. Wang, Ultrasonic cavitation: Tackling organic pollutants in wastewater, *Chemosphere* **350** (2023) 141024. <https://doi.org/10.1016/j.chemosphere.2023.141024>
- [33] R. D. Crapnell, E. Bernalte, X. Ji, C. E. Banks, Electroanalytical overview: the use of sonoelectroanalysis, *Journal of Solid State Electrochemistry* **29** (2025) 2089-2100. <https://doi.org/10.1007/s10008-024-06174-0>
- [34] P. R. Gogate, A. B. Pandit, A review of imperative technologies for wastewater treatment I: oxidation technologies at ambient conditions, *Advances in Environmental Research* **8** (2004) 501-551. [https://doi.org/10.1016/S1093-0191\(03\)00032-7](https://doi.org/10.1016/S1093-0191(03)00032-7)
- [35] H. Su, J. Sun, C. Wang, H. Wang, Study on the influence of ultrasound on the kinetic behaviour of hydrogen bubbles produced by proton exchange membrane electrolysis with water, *Ultrasonics Sonochemistry* **108** (2024) 106968. <https://doi.org/10.1016/j.ultsonch.2024.106968>